Precision Clinical Medicine, 3(1), 2020, 22–33

doi: 10.1093/pcmedi/pbz029
Advance Access Publication Date: 30 December 2019
Research Article

RESEARCH ARTICLE

Potassium channels as potential drug targets for limb wound repair and regeneration

Wengeng Zhang[1,2], Pragnya Das[3,#], Sarah Kelangi[1,2] and Marianna Bei[1,2,*]

[1]Center for Engineering in Medicine, Massachusetts General Hospital, Department of Surgery, Harvard Medical School, Boston, MA 02114, USA
[2]Shriners Hospital for Children, Boston, MA 02114, USA
[3]Center for Regenerative Developmental Biology, The Forsyth Institute, Cambridge, MA 02116, USA

*Correspondence: Marianna Bei, mbei@partners.org or mbei@mgh.harvard.edu

Abstract

Background: Ion channels are a large family of transmembrane proteins, accessible by soluble membrane-impermeable molecules, and thus are targets for development of therapeutic drugs. Ion channels are the second most common target for existing drugs, after G protein-coupled receptors, and are expected to make a big impact on precision medicine in many different diseases including wound repair and regeneration. Research has shown that endogenous bioelectric signaling mediated by ion channels is critical in non-mammalian limb regeneration. However, the role of ion channels in regeneration of limbs in mammalian systems is not yet defined.
Methods: To explore the role of potassium channels in limb wound repair and regeneration, the hindlimbs of mouse embryos were amputated at E12.5 when the wound is expected to regenerate and E15.5 when the wound is not expected to regenerate, and gene expression of potassium channels was studied.
Results: Most of the potassium channels were downregulated, except for the potassium channel *kcnj8* (Kir6.1) which was upregulated in E12.5 embryos after amputation.
Conclusion: This study provides a new mouse limb regeneration model and demonstrates that potassium channels are potential drug targets for limb wound healing and regeneration.

Key words: limb regeneration; wound healing; drug targets; potassium channels; gene expression

Introduction

Precision medicine is a medical model that customizes medical practice focusing on individual patients based on the use of genetic testing, biomarker identification, and development of targeted drugs. Identification and validation of drug targets is critical for implementation of precision medicine. Ion channels play a vital role in almost all biological processes in both health and disease and are one of six major pharmacological targets including G protein-coupled receptors, ion channels, nuclear hormone receptors, catalytic receptors, enzymes, and transporters.[1] Ion channels have served as biomarkers and therapeutic targets in many important

[#]Present address: Department of Pediatrics, Division of Neonatology, Drexel University College of Medicine, Philadelphia, PA 19102, USA
Received: 21 December 2019; **Accepted:** 22 December 2019

diseases,[2–11] such as cancers, diabetes, cardiovascular diseases, congenital blindness, cystic fibrosis, epileptic encephalopathies, pain, hypertension, wound repair and regeneration, and others.

In general, wounds heal and/or regenerate. Wound healing or wound repair results in scar tissue formation, whereas regeneration is a scar-less tissue restoration process. Regeneration is generally classified into two types: tissue and epimorphic.[12] Tissue regeneration is rapid, occurs in organs and/or tissues, such as the liver in humans, and is characterized by a lack of blastema formation. The end product is usually smaller than original and less organized. In contrast, epimorphic regeneration is slow and characterized by formation of a blastema, an aggregation of proliferating cells at wound sites. The end product is morphologically and functionally perfect.[12] A classic example of epimorphic regeneration is the limb regeneration in urodeles. The epimorphic regeneration is usually divided into three steps. First, migrating epithelial cells seal the wound site from the environment forming the wound epithelium that later thickens to form a structure known as the apical epithelial cap (AEC). This special structure provides key molecular signals needed to stimulate and maintain the early stages of regeneration.[13,14] Second, secreted matrix metalloproteinases from the wound tissue and a mass of undifferentiated mesenchymal cells beneath the AEC form a bud-like structure known as the blastema. Third, the blastema continues to grow through reciprocal interaction between the AEC and its underlying mesenchyme, resulting in regeneration of the amputated portions of the damaged tissues,[13–15] a heterogeneous collection of restricted progenitor cells.[16,17]

Limb regeneration is one of the best models of epimorphic regeneration in vertebrates as it requires blastema formation. Urodele amphibians such as newts and salamanders have exceptionally high regenerative ability and they can regenerate their limbs completely after amputation at any time during their life cycles.[12,13,18] Anuran amphibians, such as *Xenopus*, have an intermediate regenerative ability between that of urodele amphibians and other vertebrates, such as mammals. They can completely regenerate developing hindlimb buds prior to the onset of metamorphosis, but the regenerative ability declines gradually as metamorphosis proceeds.[13] Mammals, on the other hand, have a very limited regenerative ability. For example, mouse appendage regeneration is time-dependent. During embryogenesis, in a mouse younger than E14.5, wound healing is processed without scarring and appendages completely regenerate, whereas in a mouse embryo older than E14.5, a scar is formed and appendages do not regenerate.[13, 19–21] Limb amputations in mouse embryos younger than E14.5 result in blastema formation and scar-less regeneration. In contrast, in limb amputations in embryos older than E14.5, neonates, and adult mice, blastema is not formed and limbs do not regenerate, with the exception of distal limb amputations that affect digit tips.[22–24] Specifically, it has been shown that late embryonic, neonatal, and adult mice can only partially or completely regenerate their digit tips when amputation is through the distal phalanx, but they cannot regenerate when the amputation occurs at a more proximal level.[25–30] That the mouse digit tip regeneration process is similar to human distal fingertip regeneration in both children and adults suggests that study of the signaling molecules involved in regeneration and/or scar formation after limb amputation in mouse embryos could provide cues on effective regeneration stimulation and scarring suppression in humans.[13,26]

Fibroblast growth factor (FGF), Wnt/β-catenin, and bone morphogenetic protein (BMP)/Msx signaling pathways play an important role in limb regeneration and wound healing. In amputated limbs that form blastemas, FGF-8 and FGF-10 are expressed in the basal layer of the apical epithelial cap and in the underlying mesenchyme, respectively, whereas no FGF-8 and FGF-10 expression is seen in amputated limbs that lack blastema formation.[31,32] However, exogenous FGF-10 can stimulate limb regeneration in the stump of non-regenerative *Xenopus* limb buds.[33] This suggests that the signaling loop between FGF-8 and FGF-10 is critical for limb regeneration.[13] The Wnt/−catenin signaling pathway either directly or indirectly, through FGF-10 induction, regulates the early stages of limb regeneration and its function is not indispensable after blastema formation. In early limb development, BMP and its target Msx-1 are also involved in induction of apical ectodermal ridge (AER), a structure equivalent to the apical epithelial cap (AEC) during limb regeneration. In both fetal and neonatal mice, *Msx1* and *Msx2* are expressed during digit regeneration, but not during wound healing associated with proximal amputations where no regenerative response is observed.[29] When digits are amputated at a distal level in an E14.5 Msx1 mutant limb and then the limb is cultured *ex vivo* to evaluate the regeneration process, a regeneration defect is observed and this defect can be rescued in a dose-dependent manner by exogenous BMP4.[34]

Endogenous bioelectric signaling plays a critical role in cell proliferation, migration, differentiation, apoptosis, and cell cycle regulation, which are also required for development, wound healing, and regeneration.[35] Indeed, after limb amputation in salamanders, newts, and frogs, a strong, steady, and polarized bioelectric potential could be immediately measured in a proximodistal direction within the limb stump. Inhibition of this current abrogates the regeneration response and activation of this current rescues regeneration.[36–41] For example, induction of H^+ flux by V-ATPase proton channel activation in the wound of an amputated tail in a non-regenerative condition (after metamorphosis stage) leads to production of a perfect tail of the exact right size. Pharmacologic or genetic inhibition of this channel abolishes the regeneration in *Xenopus*.[38] Also, an increase of intracellular sodium is required for initiating

regeneration after *Xenopus laevis* tail amputation. Inhibition of sodium transport leads to regeneration failure. The Na1.2 sodium channel gene is absent in non-regenerative tails, while mis-expression of human Nav1.5 or pharmacologic induction of a transient sodium current can rescue regeneration even after formation of non-regenerative conditions.[37] These studies suggest that ion channels are critical for tail regeneration in *Xenopus laevis* and they may regulate regeneration either directly or through downstream pathways such as Wnt/Hedgehog/Notch, Msx1, and BMP pathways. However, the role of ion channels in limb regeneration in mammals remains largely unknown.

Potassium channels are found in all living organisms and represent the largest group of ion channels.[42] In both excitable and non-excitable cells, potassium channels regulate Ca^{2+} signaling, volume regulation, secretion, cell death, proliferation, migration, differentiation, and, identified most recently, skin wound healing.[43,44] For example, potassium channel openers and the ionophore, valinomycin, enhance skin wound healing, whereas potassium blockers delay wound healing after an acute insult of mouse skin.[45] Thus, potassium channels could be potential therapeutic targets for wound repair and regeneration.[42] In this study, we examined the gene expression of potassium channels at amputated hind limbs of mouse embryos at E12.5 and E15.5. Our experiments reveal a role for potassium channels in mouse limb regeneration and demonstrate that mouse embryos may serve as a good limb regeneration model.

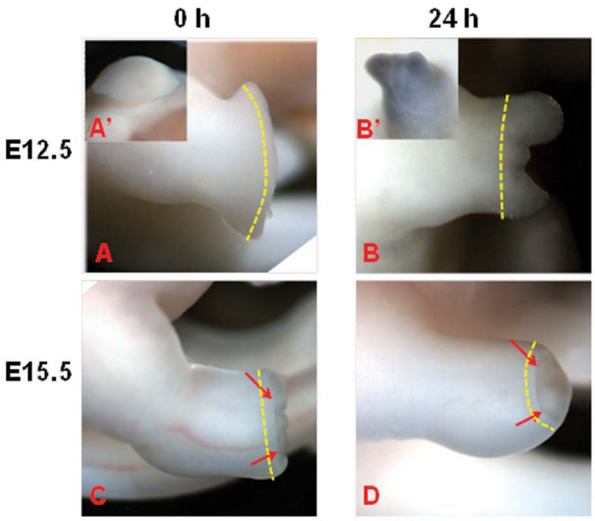

Figure 1. Regeneration and wound healing of mouse embryonic limbs. (A and A') A side view and a front view of a freshly wounded E12.5 embryonic hindlimb. The right hindlimb bud was amputated at the presumptive ankle level leaving an ovoid excisional surface without visible contraction of the skin tissues. (B and B') A side view and a front view of a representative E12.5 embryo limb 24 hours after limb amputation. The wound is completely closed and two blastema-like structures form proximodistally at the anterior and posterior sides above the wound surface. (C) Immediately after the hindlimb was severed at the ankle level at an E15.5 embryo. The skin tissues around the wound are slightly contracted (red arrows). (D) 24 hours after limb amputation in an E15.5 embryo, the skin rounds up but the wound cannot close (red arrows). Note the dotted yellow line indicates the collection of tissues close to the wound surface.

Materials and methods

Animals

BALB/c inbred mice purchased from Taconic (Ithaca, NY, USA) were kept in a conventional room with a 12-hour light-dark cycle at constant temperature and provided with standard laboratory food and water. All procedures used in this paper were approved by the MGH/IACUC (Institutional Animal Care and Use Committee).

Mouse embryo culture and limb amputation induction

The embryo culture and limb amputation procedure followed published protocols[46–48] with some modifications. Briefly, timed pregnancies were set up and the day of vaginal plug formation was regarded as embryonic day 0.5 (E0.5). Embryos were dissected from pregnant mice at the age of E12.5 and E15.5. The wounds were made by severing the hindlimb buds at the ankle level to expose a clean ovoid wound. Embryos were then transferred to round-bottom culture tubes (BD Biosciences, San Jose, CA, USA) with 4 mL of embryo culture medium (EmbryoMax® KSOM w/1/2 Amino Acids and Glucose; Millipore, Billerica, MA, USA) and put on a rotating culture station at 30 rpm in an incubator with a temperature at 37 °C and 5% CO_2. Wounded embryos were cultured for periods of 0, 6, 12, and 24 hours, and the protocol is described in detail by Zhang and Bei.[49]

Total RNA preparation

At different time points after wound induction, the embryos in culture were rinsed with DEPC-treated PBS briefly and then stored in RNAlater solution (Invitrogen). Tissues close to the wound surface (showing as a dotted yellow line in Fig. 1) were collected under a dissecting microscope. Total RNA was prepared from pooled tissues from at least five embryos using the RNeasy Mini Kit (Qiagen, Valencia, CA, USA) with on-column RNase-free DNase digestion to remove DNA contaminations. Total RNA concentration was assessed using NanoDrop 8000 spectrophotometer (Thermo Scientific, Asheville, NC, USA). Only high-quality RNA was used for the following experiments.

Quantitative real-time PCR assay

To assess the expression changes of potassium channels during wound healing at different mouse embryonic stages E12.5 and E15.5, the quantitative expression of 84 ion channel and transporter genes was analyzed using Mouse Ion Channel & transporter RT2 Profiler PCR array (Cat. number PAMM-036Z, SABiosciences,

Table 1. List of primers used for real-time PCR (F: forward primer; R: reverse primer).

kcna6/Kv1.6	F: GATCCGCTTCTATCAGTTGGG
	R: GAACTCTCCGGGTACTCAAAG
kcnb1/Kv2.1	F: ACTTGCTGAGGTTCCTGTCCT
	R: AGATGGTGACGTAGTAGGGCA
kcnc1/Kv3.1	F: ACTCAGTGACTCCCCAGATG
	R: GTGATGGAGACCAGGATGAAG
kcnc4/Kv3.4	F: GAATCGCCCATTTACTGCAAG
	R: ATCAGACAGCACCGCATTAG
kcne1/mink	F: ACCATTTAGCTACCTCTGCAC
	R: AGAACAGTCGTGGAATTGGG
kcnh2/Kv11.1	F: GATCGCCTTCTACCGGAAAG
	R: CCATGTCCTTCTCCATCACTAC
kcnj11/Kir6.2	F: CACCATTAAAGTGCCCACAC
	R: GATGCTAAACTTGGGCTTGG
kcnj15/Kir4.2-Kir1.3	F: ATGCTGGAGATGCTTCTGAG
	R: CACTCTGTAGGTCAGGAATCTTC
kcnj1/Kir1.1	F: AGATGGAAGGTGTAACATCGAGT
	R: CAGGTCAAGTACAGTTGTCCAG
kcnj6/Kir3.2	F: CTGGAGATTGTGGTCATCCTG
	R: GTAGTCAACTTCGTAGAACCCG
kcnj8/Kir6.1	F: AAGAGCATCATCCCGGAGGA
	R: CAGGTCTACCAAGGTGGTGAA
kcnk1/K2p1.1	F: GTTCCGAGAGCTGTACAAGATC
	R: AGGTCTTCGTCCTTGTCTTTC
kcnq1/Kv7.1	F: AGCACACCCCATTTCTTGAG
	R: CTACAAAGTACTGCATGCGC
kcns1/Kv9.1	F: TCAGCTTCGAGGTGTCGTC
	R: CCAGCAGTGTGAGATAGAAGGG

data not shown). Fourteen out of 39 potassium channel genes showing potentially important changes by the array assays were selected for the real-time PCR assay. Samples for each time point were collected from at least five embryos. Each time point was repeated once. To ensure gene-specific PCR products and accurate results, we designed 2–3 pairs of primers for each gene and select those giving only one sharp PCR product band at the right size for the final real-time PCR assay. The primers used in this assay for each gene are listed in Table 1.

The cDNA was synthesized from 1 μg of total RNA by random-primed reverse transcription (Transcriptor First Strand cDNA Synthesis Kit, Roche, Indianapolis, IN, USA). Real-time PCR was performed using the LightCycler 480 SYBR Green I Master kit. The Ct (cycle threshold) values were normalized to the endogenous actb expression level and then the relative expression level (REL) between the different time points was calculated using the Livak method.[50]

Western blotting

Pooled limb tissues from at least five embryos were lyzed in RIPA lysis buffer (50 mM Tris, 150 mM NaCl, 0.1% SDS, 0.5% sodium deoxycholate, and 1% NP40) with protease inhibitor tablet (Roche, Indianapolis, IN, USA). The protein concentration was measured using Bio-Rad reagents. Proteins (20 μg) were loaded to the pre-casted 4%–12% of tris-glycine gel (Lonza, Allendale, NJ, USA), and the proteins were separated at 100 V for about 100 minutes. Protein samples were then transferred onto nitrocellulose membranes (Bio-Rad, Hercules, CA, USA) at 220 mA for 3 hours at 4 °C. After being blocked, membranes were incubated with primary antibody on a rotator shaker in a cold room overnight. Blots were then incubated by a species-specific horseradish peroxidase-labeled secondary antibody and developed using chemiluminescent substrate (Pierce, Rockford, IL, USA). The actb protein expression served as an endogenous control. Primary antibodies used were: *kcna6* (Kv1.6; Alomone, Cat number APC-003, Jerusalem 91042 Israel), *kcnh2* (Kv11.1; abcam, Cat number: ab81160, Cambridge, MA, USA), *kcnj8* (Kir6.1; Sigma, Cat number: P0874, St. Louis, MO, USA), and anti-β-actin (actb; Sigma, Cat number: A2228).

Whole mount *in situ* hybridization

Embryos at 0, 6, 12, and 24 hours post-wounding were fixed in 4% paraformaldehyde in DEPC-PBS overnight at 4 °C and dehydrated for 10 minutes each in 25%, 50%, 75%, and 100% methanol in PBT (PBS with 0.1% Tween 20). The embryos were then stored in 100% methanol at −20 °C. Antisense riboprobes were labeled with digoxygenin-UTP by *in vitro* transcription with T7 RNA polymerase using a DIG RNA Labeling Kit from Roche. The probes were amplified using the following primers (forward/reverse):

kcna6: TCGTCTGGTTCACGTTTGAGC/ACGTGGGTATACTGGCCTTG.

kcnh2: GGAACAGCCTCACATGGACT/AGGCTCTCCAAAGATGTCG.

kcnj8: CTATCATGTGGTGGCTGGTG/TATCATACAGGGGGCTACGC.

Results

Wound closes and a blastema-like structure forms in E12.5 but not in E15.5 mouse embryos after limb amputation

Most studies show that limb regeneration in mice occurs only when amputation is through the distal phalanx of digits (digit tips). Chan *et al.* reported that an excision wound made in E10 mouse embryos at a more proximal level, at the base of the limb bud, could form regenerative outgrowths.[19] To establish a new regeneration limb model in mammals and to explore whether regeneration occurs when amputation occurs at a more proximal level along the limb axis, mouse hindlimbs were amputated at the ankle level in both E12.5 and 15.5 mouse embryos. We found that amputation through the ankle level in E12.5 embryos results in a regeneration response manifested by the formation of a blastema structure whereas amputation in E15.5 embryos does not. Specifically, in E12.5 embryos, excision of the hindlimb buds at the ankle

level leaves an oval-shaped wound surface and shows no contraction of the skin tissues remaining in a well-rounded shape (Fig. 1A and A'). After 6 hours of healing in an *ex vivo* culture condition, the wound margin becomes smooth and the tissues at the anterior and posterior borders start to round up. At 12 hours, the ends further round up and two blastema-like structures appear proximodistally at the anterior and posterior ends of the wound (data not shown). By 24 hours, the wound is completely closed, presented as a smooth and shining surface and the blastema-like tissues are further elongated proximodistally at the anterior and posterior sides of the amputation plane (Fig. 1B and B'). In contrast, in E15.5 embryos, after amputation, the flank tissue surrounding the site of amputation retracts back immediately and the bone protrudes slightly (Fig. 1C). During the 24 hours of culture, the skin gradually rounds up but the wound never closes (Fig. 1D). These results indicate that amputation through the ankle level in E12.5 embryos results in a regeneration response manifested by the formation of a blastema structure whereas amputation in E15.5 embryos does not.

Potassium channels are differentially expressed between E12.5 (blastema) and E15.5 (no blastema) mouse limbs after amputation

To determine whether the expression patterns of potassium channels are modified after limb amputation at the ankle level, we collected the tissue close to the wound edges from amputated limbs of E12.5 and E15.5 mouse embryos at 0, 6, 12, and 24 hours after wound induction, and performed a high throughput assay to determine the identity and level of potassium channel gene expression. t = 0 represents the time immediately after wound induction. Specifically, immediately after wounding, the mouse embryos were placed into RNAlater solution that rapidly permeated tissues to stabilize and protect cellular RNA. After that critical step allowing for immediate stabilization and protection of cellular RNA, the tissue was collected and mRNA was prepared. Thus, the mRNA level at the 0-hour time point (t = 0) should be similar to the pre-wounding level because some time is required for a new gene to be induced. A mouse ion channel and transporter PCR array was used containing, among other genes, 39 genes encoding potassium channels. After repeating the assay, 14 of those genes showed potentially remarkable changes between E12.5 (blastema) and E15.5 (no blastema) (data not shown) and were analyzed by real-time PCR. The REL of these genes, one gene in a row, at different time points after limb amputation at E12.5 (blastema) and E15.5 (no blastema) mouse embryos is shown as a heatmap in Fig. 2A.

The REL of the potassium channels at the 0 hour time point (t = 0) after limb amputation represents the basal expression level of the genes in limb tissues similar to pre-wounding level because some time is required for a new gene to be induced. *kcnj1* (Kir1.1), *kcna6*, and *kcnj11* (Kir6.2) are expressed at a much higher level at E12.5 compared to E15.5 shown as a heatmap (Fig. 2A) or a column graph (Fig. 2B). In contrast, *kcnj8*, *kcnc4* (Kv3.4), and *kcnk1* (K2p1.1) are expressed at lower levels in E12.5 compared to E15.5; all other genes show no big difference between E12.5 (blastema) and E15.5 (no-blastema). These results suggest that these genes may play different roles at different stages of embryonic limb development.

We then determined the dynamic change of REL at 6, 12, and 24 hours after limb amputation (Fig. 2A) and we specifically compared the REL at 24 hours after amputation to the REL at 0 hours after amputation [basal expression level (t = 0 hour), Fig. 2C] in E12.5 and E15.5 mouse limbs. At E12.5 amputated limbs (blastema) the REL of *kcnj1*, *kcna6*, and *kcnb1* (Kv2.1) genes was gradually reduced at 6, 12, and 24 hours (Fig. 2A) with their REL at 24 hours compared to the basal expression level (0 hour) downregulated 59.95 times for *kcnj1*, 7.51 times for *kcna6*, and 3.83 times for *kcnb1*, respectively (Fig. 2C). In contrast, in E15.5 amputated limbs (no blastema) the REL of *kcnj1*, *kcna6*, and *kcnb1* genes at 24 hours compared to the basal expression level (0 hour) is minimal, lower than 2.4 times (Fig. 2A and 2C). Interestingly, the REL of *kcnj8* gene is upregulated at 24 hours compared to the basal expression level (0 hour) by 6.23 times in E12.5 amputated limbs only (Fig. 2C). On the other hand, the REL of the *kcnh2* gene is remarkably downregulated at 24 hours compared to the basal expression level (0 hour) in both E12.5 and E15.5 after limb amputation (Fig. 2C). All other potassium genes *kcnj15* (Kir4.2-Kir1.3), *kcnc4*, *kcnj11*, *kcnk1*, *kcnc1* (Kv3.1), *kcne1* (minK), *kcnj6* (Kir3.2), *kcns1* (Kv9.1), and *kcnq1* (Kv7.1) may not be essential for either blastema or no blastema formation as their expression changes at 24 hours versus 0 hour are lower than three times (Fig. 2C).

These results demonstrate that, in contrast to all other channels in the array where no robust expression is observed at t = 0 and no remarkable, further change is observed in their relative expression level thereafter in both E12.5 (blastema) and E15.5 (no blastema) forming limbs, the potassium channels *kcnj1*, *kcna6*, *kcnb1*, and *kcnj8* behave differently suggesting that manipulation of their function may play a role in promoting blastema formation and thus regeneration.

Spatiotemporal and protein expression pattern of *kcna6*, *kcnj8*, and *kcnh2* potassium channels

To confirm the expression changes of potassium channels revealed by real-time PCR, we further performed whole mount *in situ* hybridization and Western blotting to check the localization and protein expression level of *kcna6*, *kcnj8*, and *kcnh2* genes, three representative genes of the array and real-time PCR results (Figs. 3–5). The main reasons for selecting these three genes are that they have been reported to play an important role in skin wound healing,[49] thus they are good candidates for

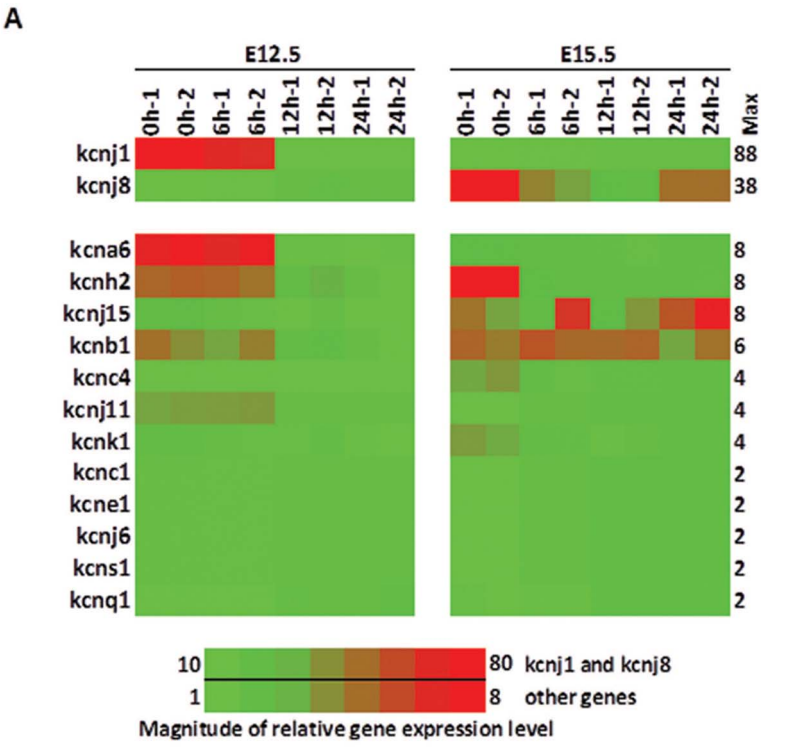

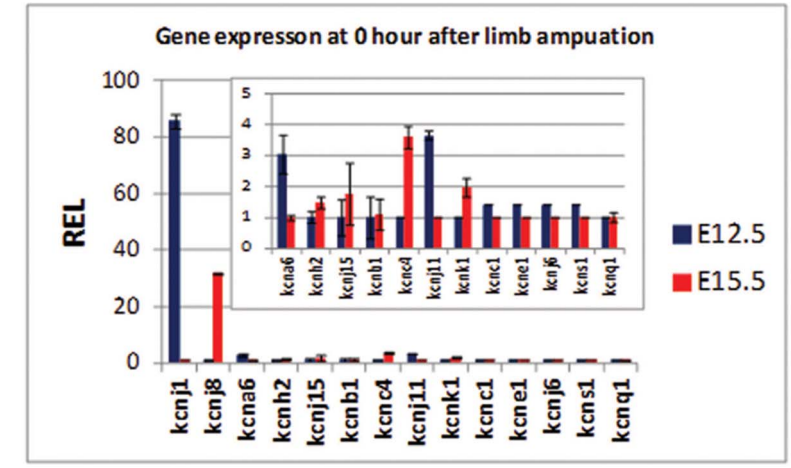

C

Gene	kcnj1	kcnj8	kcna6	kcnh2	kcnj15	kcnb1	kcnc4	kcnj11	kcnk1	kcnc1	kcne1	kcnj6	kcns1	kcnq1
E12.5	-59.93	6.23	-7.51	-4.54	-2.45	-3.83	1.01	-2.54	-1.64	1.01	1.01	1.01	1.01	1.74
E15.5	2.4	-1.74	-1.4	-4.39	1.58	-1.19	-2.12	2.4	-1.99	2.40	2.40	2.40	2.40	1.67

Figure 2. The relative expression level (REL) of 14 potassium channels during regeneration and wound healing. (A) Heatmap of the REL of potassium channels. Expression values for each gene at a row are colored from green (low) to red (high). As the expression levels of *kcnj1* and *kcnj8* (top two rows) are much higher than others, they are separated from other potassium channels to display a better color map. The leftmost column displays the gene names and the rightmost column shows the maximum changes of REL between all the different time points. Each time point was repeated once. The left half shows the REL at E12.5, and the right half at E15.5 embryos. (B) The REL of potassium channels at 0 hour after limb amputation. The values on the Y axis represent the REL between E12.5 and E15.5 limbs at 0 hour post amputation. The inset figure shows a more detailed view of the genes with a lower REL. *kcnj1*, *kcna6*, and *kcnj11* are expressed at a much higher level, whereas *kcnj8*, *kcnc4*, and *kcnk1* are expressed at a lower level in E12.5 limbs than E15.5 limbs. (C) Upregulation or downregulation of potassium channels at 24 hours versus 0 hour after limb amputation. The negative values denote downregulation, whereas the positive values represent upregulation. This shows that *kcnj1*, *kcna6*, and *kcnb1* are downregulated at E12.5 limbs, and *kcnh2* is downregulated at both E12.5 and E15.5 limbs, whereas *kcnj8* is upregulated at E12.5 limbs by three times or more. All other values are lower than three times, indicating no remarkable changes.

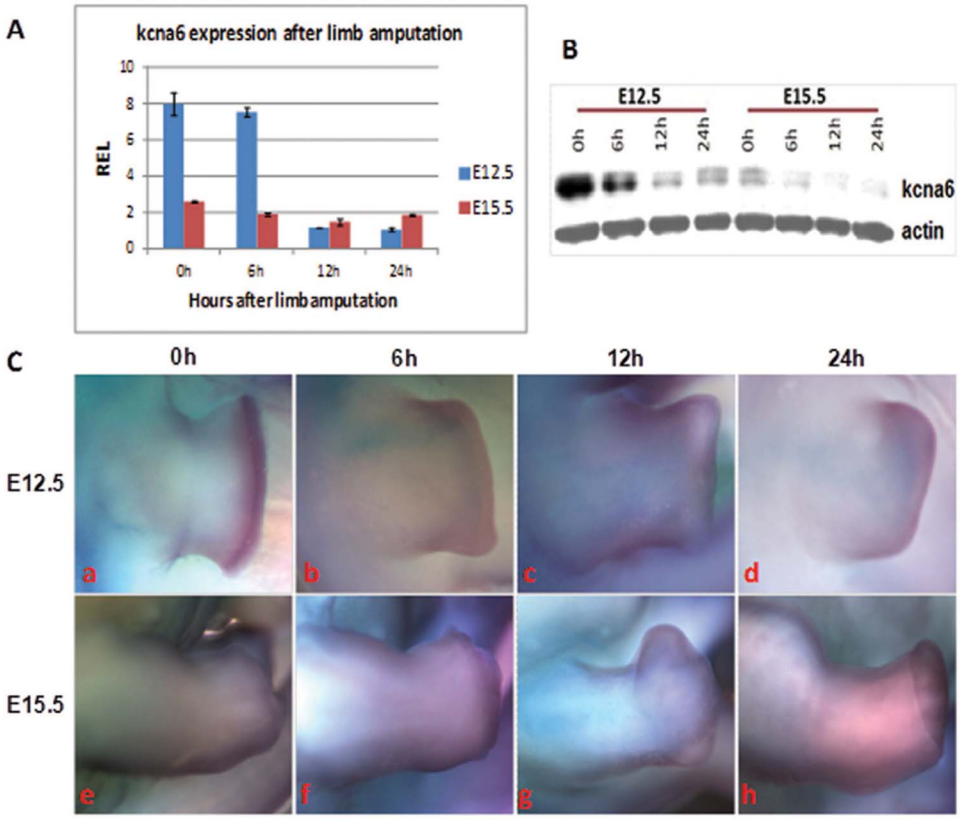

Figure 3. *kcna6*/Kv1.6 expression after limb amputation in mouse embryos. (A) Real-time PCR and (B) representative Western blotting show that the relative expression level (REL) of *kcna6* is high in E12.5 limbs and downregulated, while its expression is low in E15.5 limbs with no remarkable changes post wounding. (C) *In situ* hybridization shows that *kcna6* is highly expressed at the wound surface immediately after limb amputation at E12.5 embryos (C, a) and is rapidly reduced after wound induction (C, b-d). There is no obvious expression at E15.5 embryonic limbs (C, e–h).

further study in limb wound healing, and that only for these genes were specific antibodies available.

Based on RT-PCR results, in E12.5 limbs (blastema) the basal expression level (0 hour) of the *kcna6* gene is much higher than that in E15.5 embryos (no blastema) (Figs. 2C and 3A). At E12.5 the REL of *kcna6* gene is gradually reduced at 6 and 12 hours, and remarkably downregulated at 24 hours after amputation compared to the basal expression level (0 hour) (Fig. 3A), while at E15.5 *kcna6* is expressed at low level and shows little decrease at 6, 12, and 24 hours after amputation (Fig. 3A). Western blotting experiments were performed to test the expression pattern of *kcna6* at the protein level. The results further corroborate with the results of the real-time PCR (Fig. 3B). In addition, *in situ* hybridization experiments with probes specific for *kcna6* show that at E12.5 *kcna6* is highly expressed at the wound surface just after amputation (0 time) (Fig. 3C, a) and that this expression is downregulated thereafter at 6, 12, and 24 hours after amputation (Fig. 3C, b–d). In contrast, at E15.5 no obvious expression is observed (Fig. 3C, e–h). The qualitative expression pattern of *kcna6* at the RNA level further corroborates with the results of the real-time PCR and protein level (Fig. 3).

Similar experiments were performed for the *kcnj8* and *kcnh2* genes. As shown, the REL of the *kcnj8* gene is upregulated at 24 hours compared to the basal expression level (0 hour) at E12.5, while there is no robust change in REL at E15.5 when the gene is expressed at low levels (Figs. 2C and 4A). Western blotting experiments were performed to test the expression pattern of *kcnj8* at the protein level. The results corroborate with the results of the real-time PCR in E12.5 but not in E15.5 limbs (Fig. 4B). In addition, *in situ* hybridization experiments with probes specific for *kcnj8* show that at E12.5 *kcnj8* is expressed at low levels at the wound surface just after amputation (0 time) (Fig. 4C, a) and that this expression is upregulated thereafter at 6, 12, and 24 hours after amputation (Fig. 4C, b–d). In contrast, at E15.5 no remarkable expression is observed (Fig. 4C, e–h).

The REL of *kcnj8* mRNA at 0 hour after limb amputation appearing much higher in E15.5 than in E12.5 limbs (Fig. 4A), and the protein level appearing very low at 0 hour in both E12.5 and E15.5, at first seem contradictory. This discrepancy is possibly a result of the very low endogenous mRNA expression level of *kcnj8* gene in both E12.5 and E15.5 limbs, reflected by the high cross threshold (Ct) values from real-time PCR assays, 30–33

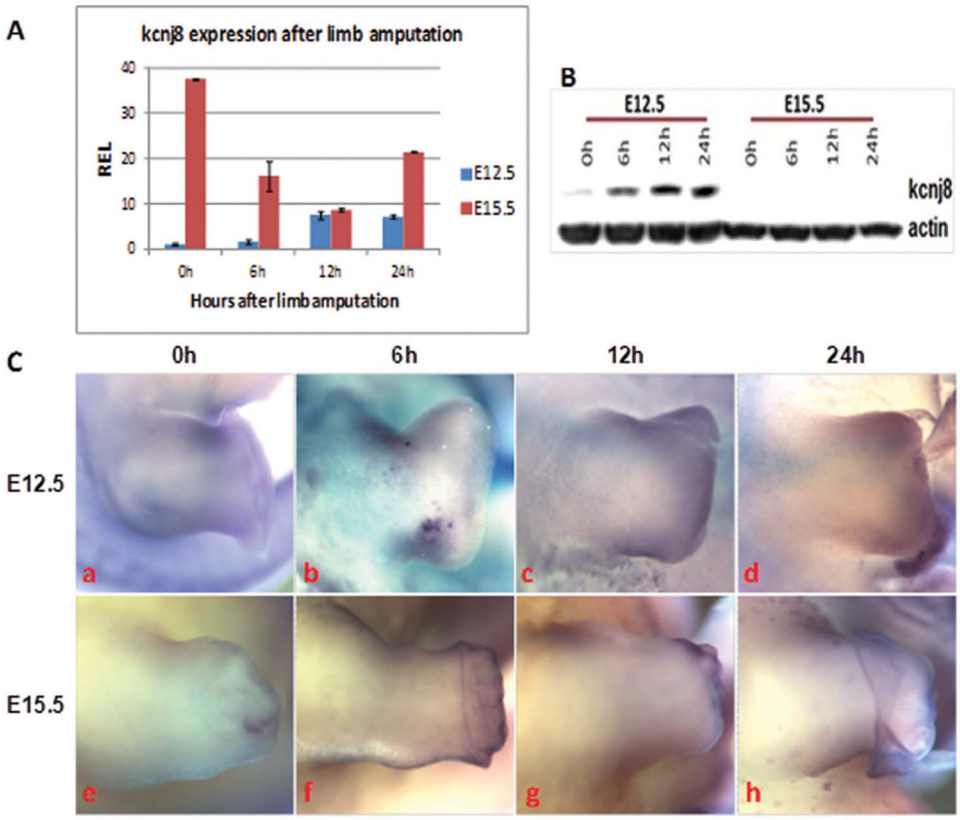

Figure 4. *kcnj8*/Kir6.1 expression after limb amputation in mouse embryos. (A) The real-time PCR shows that the relative expression level (REL) of *kcnj8* is upregulated in E12.5 limbs whereas it is downregulated in E15.5 limbs after wounding. (B) Representative Western blotting indicates that *kcnj8* is robustly induced after limb amputation at E12.5 embryos, but there is no detectable expression in E15.5 limbs, which may be a result of different post-translational modifications. (C) *In situ* hybridization shows that there is no obvious *kncj8* expression at 0 hour (C, a) at E12.5 limbs (note the blue background in the whole embryo), whereas this is visible at the wound surface at 12 and 24 hours (C, c and d) after wound induction. There was no obvious staining in E15.5 wounded limbs (C, e–h).

for E12.5 and 27.26–30.63 for E15.5 limbs. Other reasons could be genetic variation, environmental changes, and different post-translational modification between E15.5 and E12.5 embryos.[51]

The REL of the *kcnh2* gene is remarkably downregulated at 24 hours compared to the basal expression level (0 hour) in both E12.5 and E15.5 after limb amputation at mRNA and protein level (Fig. 2C; Figs. 5A and B). *In situ* hybridization also shows that *kcnh2* is highly expressed at the wound surface at 0 hour and is gradually reduced at 6, 12 and 24 hours after amputation in the E12.5 limbs (Fig. 5C, B–D). At E15.5 mouse embryos, the *kcnh2* expression is low and mostly located in skin tissues around the wound surface at 0 hour and no visible signaling at 6, 12, and 24 hours after limb amputation (Fig. 5C, E–H). The gene expression pattern detected by *in situ* hybridization (Fig. 5C) corresponds with what detected by Western blotting very well (Fig. 5B).

There is a difference between the expression level of *kcnh2* mRNA which is a little higher at E15.5 compared to E12.5 at 0 hour (Fig. 5A), with the expression level of *kcnh2* protein which is lower at E15.5 compared to E12.5 at 0 hour (Fig. 5B). This difference is most likely a result of differential post-translational modifications of *kcnh2* protein at different developmental stages.[51]

Discussion

Blastema formation at E12.5 mouse embryos after limb amputation at the ankle level: a model for studying limb regeneration

Mouse limb amputation is the most commonly used regeneration model in mammals.[18,25,26,52] Mouse limbs regenerate at all embryonic, postnatal, and adult stages if the amputation is limited to the distal tip of digits within the base of the nail, but they cannot regenerate when the amputation occurs at a more proximal level.[25–30,52] For the regeneration to occur, an initial critical regeneration step, the formation of a structure, known as blastema is required. However, blastema formation could occur even if the amputation occurs at a more proximal level than the tip of digits. For example, in E10 mouse embryos, outgrowths are observed from flank tissues at the anterior and posterior borders of the wound 24 hours after mouse forelimb buds are amputated from their base.[19] These outgrowths may differentiate into various tissues after being grafted beneath adult kidney capsules and the resulting regenerated tissues have very similar structures to a normal limb bud based on morphological and histochemical criteria. Thus, rapid wound closure by regenerative epithelium is the first step of limb

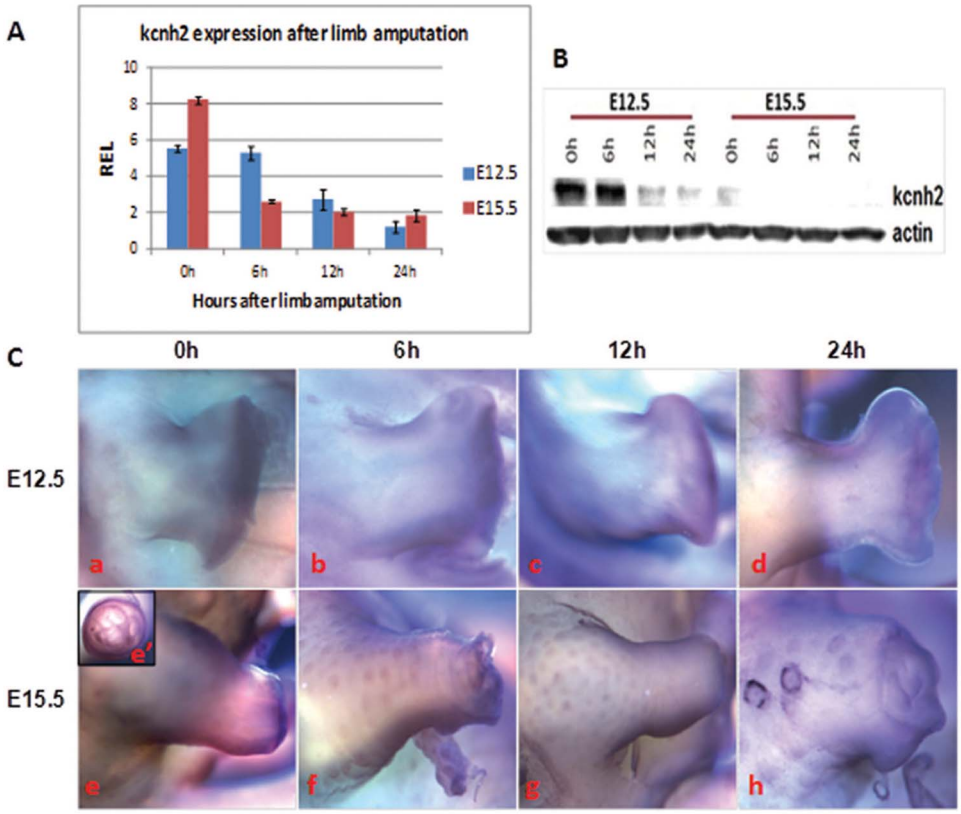

Figure 5. *kcnh2*/Kv11.1 expression after limb amputation in mouse embryos. (A) Real-time PCR shows that the relative expression level (REL) of *kcnh2* gene is high immediately after limb amputation and gradually downregulated afterwards in both E12.5 and E15.5 mouse limbs. (B) Representative Western blotting demonstrates that *kcnh2* protein is downregulated after wound induction in both E12.5 and E15.5 limbs. But the *kcnh2* protein is much lower at E15.5 limbs than E12.5, although the mRNA level is a little higher at E15.5 as shown in Fig. 4A at 0 hour. This is possibly a result of different post-translational modification of *kcnh2* protein in E12.5 and E15.5 limbs. (C) *In situ* hybridization shows that *kcnh2* is expressed at the wound surface (C, a) and reduced with time post wounding in E12.5 limbs (C, b-d). In E15.5 limbs, it is highly expressed mostly in the skin tissues of the wound surface (C, e and e', a side and wound surface view) and downregulated during wound healing (C, f–h).

regeneration that minimizes tissue damage, infection, and the inflammatory response,[53] followed by blastema formation which is the herald of the regeneration process.[25] Once a blastema is established, limb regeneration can autonomously proceed even if it is grafted to different locations of the body such as the eye chamber or dorsal fin.[13]

The present study shows that after amputation of the E12.5 mouse hindlimbs at the ankle level, the wounded limbs form two outgrowths, blastema structures, at the anterior and posterior sites above the wound surface (Fig. 1B). These results further indicate that blastema formation can occur even if the amputation occurs at a more proximal level than the digit tip, and, as in E10 mouse embryos, an E12.5 limb ankle-level amputation model could be used to assess limb regeneration.

In our study, during the 24-hour culture of the amputated-ankle-level E12.5 mouse embryos, blastemas formed gradually following wound closure by epithelial cells. In vertebrate limbs, signaling from the proximodistal (PD), anteroposterior (AP), and dorsoventral (DV) axes is critical for limb development.[54,55] On the other hand, it has been demonstrated that lineage-restricted tissue stem cells and not pluripotent blastema cells are the cells responsible for limb regeneration after amputation, mimicking the digit growth during development.[26] Thus, after limb amputation at the ankle level, the signaling from proximodistal, dorsoventral, and anteroposterior axes may be required for limb development but it is only the lineage-specific tissue stem cells that may partially account for the blastema-like outgrowth formation in E12.5 mouse embryos reported here. Although BMP/Msx, Wnt/β-catenin, and FGFs are reported to be needed for regeneration[29,37] and CD31-positive endothelial and SCA-1-positive stem cells are reduced in blastemas in comparison to surrounding connective tissues and bone marrow cells,[27] the truth of the matter is that there are still no defined biomarkers for blastema tissue formation. Therefore, it would be very interesting to further characterize the cellular and molecular mechanisms involved in the blastema-like structure formation process in the newly defined E12.5 limb regeneration model.

Role of potassium channels in the limb regeneration process

As mentioned before, non-mammals (such as urodeles) completely regenerate limbs as adults, whereas mammals (such as mice) can regenerate only digit tips. In addition, endogenous bioelectric signaling mediated by ion channels plays a critical role in the non-mammalian limb regeneration process. However, the role of ion channels in regeneration of mammalian limbs is not yet defined. Recent studies have provided evidence that potassium channels may mediate skin wound healing and regeneration interactively in mice.[49] Here, using our mouse limb regeneration model, we report that four potassium genes are differentially expressed between E12.5 (blastema formed) and E15.5 (blastema is not formed) amputated limbs, suggesting that potassium channels are regulated during both development and regeneration. After limb amputation, *kcnj1*, *kcna6*, and *kcnb1* are downregulated in E12.5 compared to E15.5 limbs, while *kcnj8* is upregulated in E12.5. Potassium channels usually conduct potassium ions out of cells, except for kcnj8 which allows potassium to flow into cells. Any change in their relative expression over time in response to an insult (wound induction) would lead to inhibition of (K^+) ions conducted out or inside of the border cells, and eventually to loss of plasma membrane potential equilibrium (PMP) and depolarization. Consistently, previous reports have demonstrated that depolarization participates in regeneration and wound healing.[35,56–60] For example, *in vitro* bovine corneal endothelial cell wound healing occurs through actin cable formation and cell migration into the injured area.[56] Interestingly, membrane potential depolarization occurs at the leading edge of the migrating cells and the depolarization gradually extends into the neighboring cells.[56,57] In a planarian head regeneration model, Beane *et al*. discovered that H,K-ATPase activity is required for depolarization of the regenerating anterior blastema, and the depolarization itself is sufficient to drive ectopic anterior regeneration. This indicates that membrane voltage is a key initiator of head formation during regeneration.[59] Lotz *et al*. also reported that inhibition of potassium channels by small molecules accelerates *in vitro* intestinal epithelial cell wound healing while stimulation of these channels has no effect on the healing rate.[61] We recently reported that potassium channels *kcnh2* and *kcnj8* interactively regulate wound healing and regeneration in a wound made in mouse embryo skin or cultured JB6 epidermal sheets, further highlighting the role of dynamic modification of cell membrane potentials in clinical wound healing therapy.[49]

In conclusion, this study offers a new limb regeneration model in E12.5 mouse embryos and has for the first time documented the expression changes of 14 endogenous potassium channels during regeneration and wound healing in mammalian limb amputation models. The results suggest that potassium channels may serve as potential drug targets for wound repair and regeneration.

Acknowledgements

This work was supported by the National Institutes of Health (NIH) /National Institute of Dental and Craniofacial Research (NIDCR) (Grants No. 3R01DE027255-01S1 and 1R21DE028091-01).

Conflict of interest

None declared.

References

1. Alexander SPH, Mathie A, Peters JA, *et al*. The concise guide to pharmacology 2019/20: Ion channels. *Br J Pharmacol* 2019;**176** Suppl 1:S142–S228. doi: 10.1111/bph.14749.
2. Levin M, Selberg J, Rolandi M. Endogenous bioelectrics in development, cancer, and regeneration: drugs and bioelectronic devices as electroceuticals for regenerative medicine. *iScience* 2019;**22**:519–33. doi: 10.1016/j.isci.2019.11.023.
3. Abdul Kadir L, Stacey M, Barrett-Jolley R. Emerging roles of the membrane potential: action beyond the action potential. *Front Physiol* 2018;**9**:1661. doi: 10.3389/fphys.2018.01661.
4. Haustrate A, Hantute-Ghesquier A, Prevarskaya N, *et al*. Monoclonal antibodies targeting ion channels and their therapeutic potential. *Front Pharmacol* 2019;**10**:606. doi: 10.3389/fphar.2019.00606.
5. Weise-Cross L, Resta TC, Jernigan NL. Redox regulation of ion channels and receptors in pulmonary hypertension. *Antioxid Redox Signal* 2019;**31**:898–915. doi: 10.1089/ars.2018.7699.
6. Ma RSY, Kayani K, Whyte-Oshodi D, *et al*. Voltage gated sodium channels as therapeutic targets for chronic pain. *J Pain Res* 2019;**12**:2709–22. doi: 10.2147/JPR.S207610.
7. Selvaraj C, Selvaraj G, Kaliamurthi S, *et al*. Ion channels as therapeutic targets for type 1 diabetes mellitus. *Curr Drug Targets* 2019. doi: 10.2174/1389450119666190920152249.
8. Yee NS. TRPM8 ion channels as potential cancer biomarker and target in pancreatic cancer. *Adv Protein Chemistry Struct Biol* 2016;**104**:127–55. doi: 10.1016/bs.apcsb.2016.01.001.
9. Maljevic S, Reid CA, Petrou S. Models for discovery of targeted therapy in genetic epileptic encephalopathies. *J Neurochem* 2017;**143**:30–48. doi: 10.1111/jnc.14134.
10. Gentzsch M, Mall MA. Ion channel modulators in cystic fibrosis. *Chest* 2018;**154**:383–93. doi: 10.1016/j.chest.2018.04.036.
11. Shahi PK, Hermans D, Sinha D, *et al*. Gene augmentation and Readthrough rescue Channelopathy in an iPSC-RPE model of congenital blindness. *Am J Hum Genet* 2019;**104**:310–8. doi: 10.1016/j.ajhg.2018.12.019.
12. Masaki H, Ide H. Regeneration potency of mouse limbs. *Dev Growth Differ* 2007;**49**:89–98. doi: 10.1111/j.1440-169X.2007.00909.x.
13. Yokoyama H. Initiation of limb regeneration: the critical steps for regenerative capacity. *Dev Growth Differ* 2008;**50**: 13–22. doi: 10.1111/j.1440-169X.2007.00973.x.
14. Whited JL, Tabin CJ. Limb regeneration revisited. *J Biol* 2009; **8**:5. DOI:10.1186/jbiol105.
15. Stewart S, Tsun ZY. Izpisua Belmonte JC. A histone demethylase is necessary for regeneration in zebrafish. *Proc Natl Acad Sci U S A* 2009;**106**:19889–94. doi: 10.1073/pnas.0904132106.

16. Kragl M, Knapp D, Nacu E, *et al*. Cells keep a memory of their tissue origin during axolotl limb regeneration. *Nature* 2009;**460**:60–5. doi: 10.1038/nature08152.
17. Gerber T, Murawala P, Knapp D, *et al*. Single-cell analysis uncovers convergence of cell identities during axolotl limb regeneration. *Science* 2018;**362**. doi: 10.1126/science.aaq0681.
18. Ide H. Bone pattern formation in mouse limbs after amputation at the forearm level. *Dev Dyn* 2012;**241**:435–41. doi: 10.1002/dvdy.23728.
19. Chan WY, Lee KK, Tam PP. Regenerative capacity of forelimb buds after amputation in mouse embryos at the early-organogenesis stage. *J Exp Zool* 1991;**260**:74–83. doi: 10.1002/jez.1402600110.
20. Mazzalupo S, Wong P, Martin P, *et al*. Role for keratins 6 and 17 during wound closure in embryonic mouse skin. *Dev Dyn* 2003;**226**:356–65. doi: 10.1002/dvdy.10245.
21. Boglev Y, Wilanowski T, Caddy J, *et al*. The unique and cooperative roles of the grainy head-like transcription factors in epidermal development reflect unexpected target gene specificity. *Dev Biol* 2011;**349**:512–22. doi: 10.1016/j.ydbio.2010.11.011.
22. Ting SB, Caddy J, Hislop N, *et al*. A homolog of drosophila grainy head is essential for epidermal integrity in mice. *Science* 2005;**308**:411–3. doi: 10.1126/science.1107511.
23. Caddy J, Wilanowski T, Darido C, *et al*. Epidermal wound repair is regulated by the planar cell polarity signaling pathway. *Dev Cell* 2010;**19**:138–47. doi: 10.1016/j.devcel.2010.06.008.
24. Martin P. Wound healing-aiming for perfect skin regeneration. *Science* 1997;**276**:75–81.
25. Lehoczky JA, Robert B, Tabin CJ. Mouse digit tip regeneration is mediated by fate-restricted progenitor cells. *Proc Natl Acad Sci U S A* 2011;**108**:20609–14. doi: 10.1073/pnas.1118017108.
26. Rinkevich Y, Lindau P, Ueno H, *et al*. Germ-layer and lineage-restricted stem/progenitors regenerate the mouse digit tip. *Nature* 2011;**476**:409–13. doi: 10.1038/nature10346.
27. Fernando WA, Leininger E, Simkin J, *et al*. Wound healing and blastema formation in regenerating digit tips of adult mice. *Dev Biol* 2011;**350**:301–10. doi: 10.1016/j.ydbio.2010.11.035.
28. Borgens RB. Mice regrow the tips of their foretoes. *Science* 1982;**217**:747–50.
29. Reginelli AD, Wang YQ, Sassoon D, *et al*. Digit tip regeneration correlates with regions of Msx1 (Hox 7) expression in fetal and newborn mice. *Development* 1995;**121**:1065–76.
30. Neufeld DA, Zhao W. Bone regrowth after digit tip amputation in mice is equivalent in adults and neonates. *Wound Repair Regen* 1995;**3**:461–6. doi: 10.1046/j.1524-475X.1995.30410.x.
31. Christen B, Slack JM. FGF-8 is associated with anteroposterior patterning and limb regeneration in Xenopus. *Dev Biol* 1997;**192**:455–66. doi: 10.1006/dbio.1997.8732.
32. Yokoyama H, Yonei-Tamura S, Endo T, *et al*. Mesenchyme with fgf-10 expression is responsible for regenerative capacity in Xenopus limb buds. *Dev Biol* 2000;**219**:18–29. doi: 10.1006/dbio.1999.9587.
33. Yokoyama H, Ide H, Tamura K. FGF-10 stimulates limb regeneration ability in Xenopus laevis. *Dev Biol* 2001;**233**:72–9. doi: 10.1006/dbio.2001.0180.
34. Han M, Yang X, Farrington JE, *et al*. Digit regeneration is regulated by Msx1 and BMP4 in fetal mice. *Development* 2003;**130**:5123–32. doi: 10.1242/dev.00710.
35. Levin M. Molecular bioelectricity in developmental biology: New tools and recent discoveries: Control of cell behavior and pattern formation by transmembrane potential gradients. *Bioessays* 2012;**34**:205–17. doi: 10.1002/bies.201100136.
36. Jenkins LS, Duerstock BS, Borgens RB. Reduction of the current of injury leaving the amputation inhibits limb regeneration in the red spotted newt. *Dev Biol* 1996;**178**:251–62. doi: 10.1006/dbio.1996.0216.
37. Tseng AS, Beane WS, Lemire JM, *et al*. Induction of vertebrate regeneration by a transient sodium current. *J Neurosci* 2010;**30**:13192–200. doi: 10.1523/JNEUROSCI.3315-10.2010.
38. Adams DS, Masi A, Levin M. H^+ pump-dependent changes in membrane voltage are an early mechanism necessary and sufficient to induce Xenopus tail regeneration. *Development* 2007;**134**:1323–35. doi: 10.1242/dev.02812.
39. Borgens RB, Vanable JW Jr, Jaffe LF. Bioelectricity and regeneration: Large currents leave the stumps of regenerating newt limbs. *Proc Natl Acad Sci U S A* 1977;**74**:4528–32.
40. Borgens RB, Vanable JW Jr, Jaffe LF. Bioelectricity and regeneration. I. Initiation of frog limb regeneration by minute currents. *J Exp Zool* 1977;**200**:403–16. doi: 10.1002/jez.1402000310.
41. Altizer AM, Stewart SG, Albertson BK, *et al*. Skin flaps inhibit both the current of injury at the amputation surface and regeneration of that limb in newts. *J Exp Zool* 2002;**293**:467–77. doi: 10.1002/jez.10141.
42. Girault A, Brochiero E. Evidence of K^+ channel function in epithelial cell migration, proliferation, and repair. *Am J Physiol Cell Physiol* 2014;**306**:C307–19. doi: 10.1152/ajpcell.00226.2013.
43. Wulff H, Castle NA, Pardo LA. Voltage-gated potassium channels as therapeutic targets. *Nat Rev Drug Discov* 2009;**8**:982–1001. doi: 10.1038/nrd2983.
44. Jehle J, Schweizer PA, Katus HA, *et al*. Novel roles for hERG K(+) channels in cell proliferation and apoptosis. *Cell Death Dis* 2011;**2**:e193. doi: 10.1038/cddis.2011.77.
45. Denda M, Tsutsumi M, Inoue K, *et al*. Potassium channel openers accelerate epidermal barrier recovery. *Br J Dermatol* 2007;**157**:888–93. doi: 10.1111/j.1365-2133.2007.08198.x.
46. Brock J, McCluskey J, Baribault H, *et al*. Perfect wound healing in the keratin 8 deficient mouse embryo. *Cell Motil Cytoskeleton* 1996;**35**:358–66. doi: 10.1002/(sici)1097-0169(1996)35:4<358::aid-cm7>3.0.co;2-2.
47. McCluskey J, Martin P. Analysis of the tissue movements of embryonic wound healing-DiI studies in the limb bud stage mouse embryo. *Dev Biol* 1995;**170**:102–14. doi: 10.1006/dbio.1995.1199.
48. Hopkinson-Woolley J, Hughes D, Gordon S, *et al*. Macrophage recruitment during limb development and wound healing in the embryonic and foetal mouse. *J Cell Sci* 1994;**107** (Pt 5):1159–67.
49. Zhang W, Bei M. Kcnh2 and Kcnj8 interactively regulate skin wound healing and regeneration. *Wound Repair Regen* 2015;**23**:797–806. doi: 10.1111/wrr.12347.
50. Livak KJ, Schmittgen TD. Analysis of relative gene expression data using real-time quantitative PCR and the 2(−Delta C(T)) method. *Methods* 2001;**25**:402–8. doi: 10.1006/meth.2001.1262.
51. Chick JM, Munger SC, Simecek P, *et al*. Defining the consequences of genetic variation on a proteome-wide scale. *Nature* 2016;**534**:500–5. doi: 10.1038/nature18270.

52. Yu L, Han M, Yan M, *et al*. BMP signaling induces digit regeneration in neonatal mice. *Development* 2010;**137**:551–9. doi: 10.1242/dev.042424.
53. Han M, Yang X, Taylor G, *et al*. Limb regeneration in higher vertebrates: Developing a roadmap. *Anat Rec B New Anat* 2005;**287**:14–24. doi: 10.1002/ar.b.20082.
54. Towers M, Tickle C. Growing models of vertebrate limb development. *Development* 2009;**136**:179–90. doi: 10.1242/dev.024158.
55. Benazet JD, Zeller R. Vertebrate limb development: Moving from classical morphogen gradients to an integrated 4-dimensional patterning system. *Cold Spring Harb Perspect Biol* 2009;**1**:a001339. doi: 10.1101/cshperspect.a001339.
56. Chifflet S, Hernandez JA, Grasso S. A possible role for membrane depolarization in epithelial wound healing. *Am J Physiol Cell Physiol* 2005;**288**:C1420–30. doi: 10.1152/ajpcell.00259.2004.
57. Chifflet S, Hernandez JA. The plasma membrane potential and the organization of the actin cytoskeleton of epithelial cells. *Int J Cell Biol* 2012;**2012**:121424. doi: 10.1155/2012/121424.
58. Seifert JL, Desai V, Watson RC, *et al*. Normal molecular repair mechanisms in regenerative peripheral nerve interfaces allow recording of early spike activity despite immature myelination. *IEEE Trans Neural Syst Rehabil Eng* 2012;**20**:220–7. doi: 10.1109/TNSRE.2011.2179811.
59. Beane WS, Morokuma J, Adams DS, *et al*. A chemical genetics approach reveals H,K-ATPase-mediated membrane voltage is required for planarian head regeneration. *Chem Biol* 2011;**18**:77–89. doi: 10.1016/j.chembiol.2010.11.012.
60. Chifflet S, Justet C, Hernandez JA, *et al*. Early and late calcium waves during wound healing in corneal endothelial cells. *Wound Repair Regen* 2012;**20**:28–37. doi: 10.1111/j.1524-475X.2011.00749.x.
61. Lotz MM, Wang H, Song JC, *et al*. K^+ channel inhibition accelerates intestinal epithelial cell wound healing. *Wound Repair Regen* 2004;**12**:565–74. doi: 10.1111/j.1067-1927.2004.012509.x.